

# Enhanced electrophoretic mobility of nematic dipolar Janus colloids

Dinesh Kumar Sahu, and Surajit Dhara\*

*School of Physics, University of Hyderabad, Hyderabad 500 046, India*

(Dated: May 30, 2022)

We study electrophoretic mobility of metal-dielectric Janus particles with dipolar director profile in two nematic liquid crystals (LCs) having same (positive) conductivity anisotropy and opposite dielectric anisotropy. The applied ac electric field is parallel and perpendicular to the director for the positive and negative dielectric anisotropy LCs, respectively. The velocity of the Janus particles in both LCs is significantly higher than that of the non-Janus particles. We map the electroosmotic flow fields surrounding the particles using microparticle image velocimetry ( $\mu$ -PIV) and show that the flows on the metal hemisphere is stronger than that of the dielectric hemisphere and the pumping of LC along the direction of motion of the Janus particles is more than that of the non-Janus particles. For a given liquid crystal, particles with asymmetric surface properties is useful for enhancing their electrophoretic mobility and activity.

## I. INTRODUCTION

Creating active particles and studying their self-propelled or driven motility due to the external force fields have been a subject of current interest [1–7]. The collective dynamics in dense systems of such particles are fundamentally important from the active matter perspectives [8, 9]. These particles move at the expense of consumed energy and the system is far from the equilibrium [10–13]. Usually, active particles are studied in isotropic solvent like water and the particles are mostly driven externally by light or electric or magnetic fields, depending on the choice of the particles [1]. The transport of particles by electric fields in fluids is known as electrophoresis and this phenomena has been utilised in many applications such as macro-molecular sorting, display devices and colloidal assembly [14–18]. Electrophoresis is either linear or nonlinear depending on the charge and the shape polarity of the particles. In linear electrophoresis the charge particles move opposite to the direction of the electric field and the velocity varies linearly with the field ( $v \propto E$ ). In nonlinear electrophoresis or the so called induced-charge electrophoresis the motility of the particles is independent of polarity of the applied electric field and the propelling velocity is proportional to the square of the electric field ( $v \propto E^2$ ) [19–26].

The mobility of particles in nematic liquid crystals due to the electrophoresis is more intricate than that of its isotropic counter part and known as liquid crystal enabled electrophoresis (LCEEP) [27–29]. Here, the electrophoresis is nonlinear and the mobility depends on the defect structure, in particular, the surrounding director ( $\hat{n}$ , direction of the average molecular orientation) distortions as well as the anisotropic dielectric and conductivity anisotropies of the LCs [30–33]. It has been shown that for particles with quadrupolar director structure,

namely the Saturn-ring and boojum particles are non-motile due to the fore-aft symmetry of the surrounding electroosmotic flows [34]. This symmetry is however broken for a particle with point defect (dipolar particle) and the particle can move along the director. Very recently we have shown that the metal-dielectric Janus particles with quadrupolar director structure can be transported and the direction of motion can be controlled by changing the amplitude and the frequency of the applied field [35–37].

In this paper we report experimental studies on the mobility of dipolar Janus particles in two nematic liquid crystals with positive and negative dielectric anisotropies. We show that the mobility of the Janus particles in both nematic LCs is much higher than that of the non-Janus particles. We map the surrounding flow fields using the  $\mu$ -PIV technique and show that not only the fore-aft symmetry of the flow field is broken but also the flow on the metal hemisphere is stronger than that on the dielectric hemisphere.

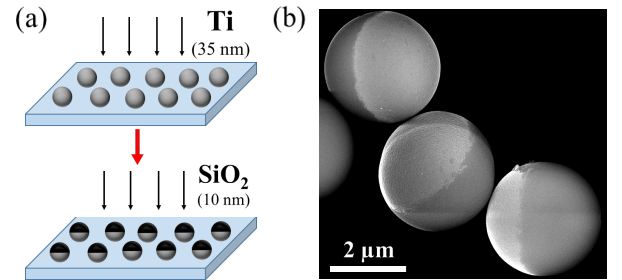


FIG. 1. (a) Diagram showing coating method of Titanium (Ti) using an electron beam deposition on silica microspheres. (b) Scanning electron microscope (SEM) image of a few Janus particles. The brighter (darker) region represents the metal (silica) hemisphere.

\* Corresponding author: sdsp@uohyd.ernet.in

## II. EXPERIMENT

Metal-dielectric Janus particles are prepared using normal deposition of Titanium (Ti) onto dry silica particles ( $\text{SiO}_2$ ) of diameter  $2a = 3.0 \pm 0.2 \mu\text{m}$  (Bangs Laboratories, USA) [16]. At first, the surface of a glass slide is made hydrophilic by treating with Piranha solution (Conc.  $\text{H}_2\text{SO}_4 : \text{H}_2\text{O}_2 :: 1 : 3$ ) for 3-4 hours and then sonicated and rinsed with distilled water. Approximately 0.1 – 1 wt% solution of the microspheres are spread over an inclined ( $45^\circ$ ) glass slide such that the solution flows down the slide leaving a monolayer of particles. After drying the slide, a thin layer ( $\sim 35 \text{ nm}$ ) of Ti is coated on the monolayer by an electron beam deposition method such that only the exposed upper hemisphere of the particles get coated (Fig.1(a)). Further, a thin layer ( $\sim 10 \text{ nm}$ ) of  $\text{SiO}_2$  is coated in order to make the surface of the particles chemically homogeneous. Then the particles are separated from the glass slides through ultrasonication for 1 – 2 minutes and washed thoroughly. The scanning electron microscope (SEM) image of a few Janus particles are shown in Fig.1(b)).

Finally, the surface of the Janus particles is treated with N, N-dimethyl-N-octadecyl-3 aminopropyltrimethoxysilyl chloride (DMOAP) in order to induce perpendicular (homeotropic) anchoring of the liquid crystal director [38, 39]. A small quantity (0.1 wt%) of DMOAP coated Janus particles is dispersed in nematic liquid crystals. We used two nematic liquid crystals, namely 5CB (pentyl cyanobiphenyl) and MLC-6608 (LC mixture obtained from Merck) and worked at the room temperature. The dielectric anisotropy of 5CB is positive ( $\Delta\epsilon = \epsilon_{\parallel} - \epsilon_{\perp} = 13$ , where  $\epsilon_{\parallel}$  and  $\epsilon_{\perp}$  are the dielectric permittivities for electric field  $\mathbf{E}$ , parallel and perpendicular to  $\hat{\mathbf{n}}$ ) whereas the same for MLC-6608 is negative ( $\Delta\epsilon = -3.8$ )[40]. For particle image velocimetry ( $\mu\text{-PIV}$ ) we dispersed CdSe/ZnS quantum dots ( $\sim 0.05 \text{ wt\%}$ ) in 5CB, using vortex mixing and ultrasonication.

We prepared Hele-Shaw type cells made of two parallel plates. Both upper and bottom plates were coated with AL-1254, cured at  $180^\circ\text{C}$  for 1h and rubbed antiparallel way for obtaining planar alignment of the director. For applying in-plane electric field (parallel to  $\hat{\mathbf{n}}$  for 5CB) the bottom plate was indium-tin-oxide (ITO) coated in which a small strip of width 2.0 mm is etched as shown schematically in Fig. 2(a). For applying electric field orthogonal to  $\hat{\mathbf{n}}$  (for MLC-6608) two ITO coated glass plates were used as shown in Fig. 4(a). A function generator (Model: Tektronix AFG31000) and a voltage amplifier (Model: TEGAM 2350) were used for applying ac electric field to the cells. The mixture (0.1wt% of Janus particles in LCs) is inserted into the cells via capillary action. An inverted optical polarizing microscope (Ti-U, Nikon) was used for the experiments. The motion of the particles was

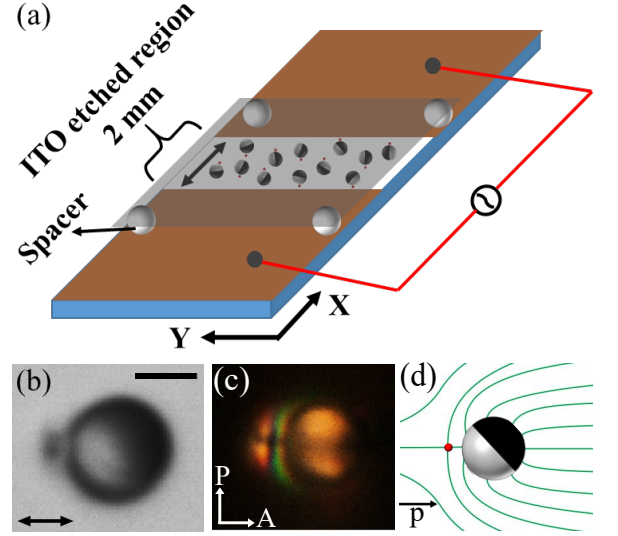


FIG. 2. (a) Diagram of a cell with in-plane electrodes. Double headed arrow indicates the director  $\hat{\mathbf{n}}$ , as well as the direction of the applied ac electric field. (b) Optical micrograph and (c) polarising optical micrograph of a dipolar Janus particle in 5CB. Double headed arrow indicates the director. Scale bar:  $2 \mu\text{m}$ . (d) Dipolar director profile around a Janus particle.  $\vec{p}$  denotes the direction of the elastic dipole.

video recorded using a  $60\times$  water immersion microscope objective (NIR Apo, Nikon) and a charge-coupled device (CCD) camera (iDs-UI) at the rate of 40 frames per second. The positions of the particles were tracked from the recorded videos using a particle tracking program.

## III. RESULTS AND DISCUSSION

The DMOAP coated Janus particles induce a hyperbolic hedgehog defect in the nematic liquid crystal and the resulting director profile is dipolar as shown in Fig.2(d). A bright field image of a dipolar Janus particle in 5CB is shown in Fig.2(b). In the transmitted light the metal coated hemisphere appears darker. The corresponding cross polarized image is also shown in Fig.2(c). When the ac electric field is applied, above a threshold field, the particles start moving along the director, keeping the point defect behind, i.e., the direction of motion is parallel to the elastic dipole  $\vec{p}$  (see Figs. 3(a-d) and Movie S1) [40]. It may be mentioned that this observation is very much different than the multidirectional mobility of the quadrupolar Janus particles in which the mobility is not restricted along the director. In particular, the direction of motion for quadrupolar particles depends on the orientation of the metal hemisphere with respect to the director [35, 36].

Figure 3(e) shows that the velocity of the Janus particles varies quadratically with the field as expected in liquid crystal enabled electrophoresis (LCEEP) [28]. For

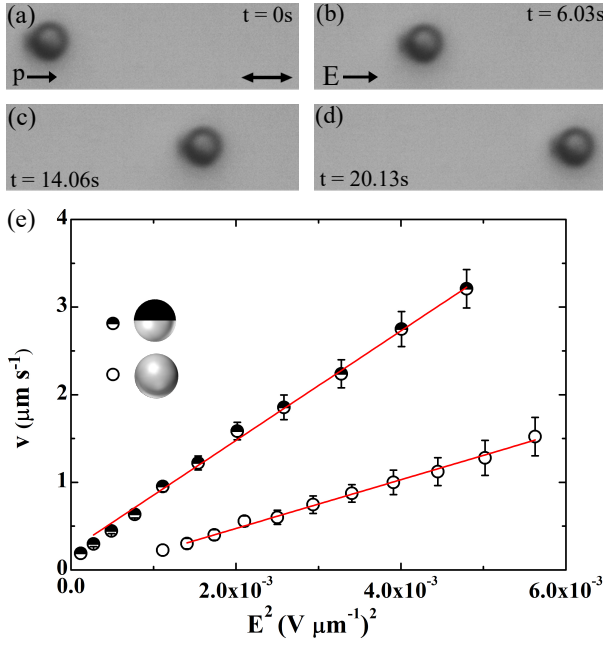


FIG. 3. (a-d) Sequence of images with elapse time showing mobility of a dipolar Janus particle along the director (see Movie S1). Note that the direction of motion is parallel to the elastic dipole  $\vec{p}$ . Double headed black arrow in (a) represents the director,  $\hat{n}$ . (e) Electric field dependent velocity ( $v$ ) of a Janus and a non-Janus particle. Red lines represent linear fits to  $v \propto E^2$  with slopes  $625$  and  $278 \mu\text{m}^3 \text{s}^{-1} \text{V}^{-2}$  for the Janus and the non-Janus particles, respectively. Error bars show the standard deviation of the mean value.

the comparative study, we have also presented the field dependent velocity of a non-Janus dipolar particle. We observe that the Janus particle moves faster than the non-Janus particle (Fig. 3(e)). For example, at  $E^2 = 4 \times 10^{-3} (\text{V}/\mu\text{m})^2$ , the velocities of the Janus and non-Janus particles are  $v_J = 2.8 \mu\text{m}/\text{s}$  and  $v = 1.03 \mu\text{m}/\text{s}$ , respectively i.e., the velocity of the Janus particles is almost double than that of the non-Janus particles in 5CB LC. It is also observed that the threshold field (above which the particles start moving) for the Janus particles is less compared to the non-Janus particles. For example, the threshold field for the Janus and non-Janus particles are measured as  $E_0 = 1.1 \times 10^{-4} \text{ V}/\mu\text{m}$  and  $E_0 = 1.1 \times 10^{-3} \text{ V}/\mu\text{m}$ , respectively.

The electroosmotic velocity of the LCs varies quadratically with the electric field and can be written as [34, 41]:

$$u = CE^2 \quad (1)$$

where the constant  $C$  is given by

$$C = \alpha \frac{\epsilon_0 \bar{\epsilon} R}{\eta} \left( \frac{\Delta\epsilon}{\bar{\epsilon}} - \frac{\Delta\sigma}{\bar{\sigma}} \right). \quad (2)$$

Here  $R$  is the radius of the particle,  $\eta$  is the viscosity and the coefficient  $\alpha \simeq 1$  [34]. The sign of the quantity in the parenthesis determines the direction of motion

of the particle with respect to the orientation of the elastic dipole  $\vec{p}$  [41]. If this quantity is negative, the direction of motion is parallel and if it is positive, the direction of motion is antiparallel to  $\vec{p}$ . For 5CB, we have measured these parameters and estimated  $\Delta\epsilon/\bar{\epsilon} - \Delta\sigma/\bar{\sigma} = -0.44$  [40]. Hence, the direction of motion is parallel to  $\vec{p}$  as expected.

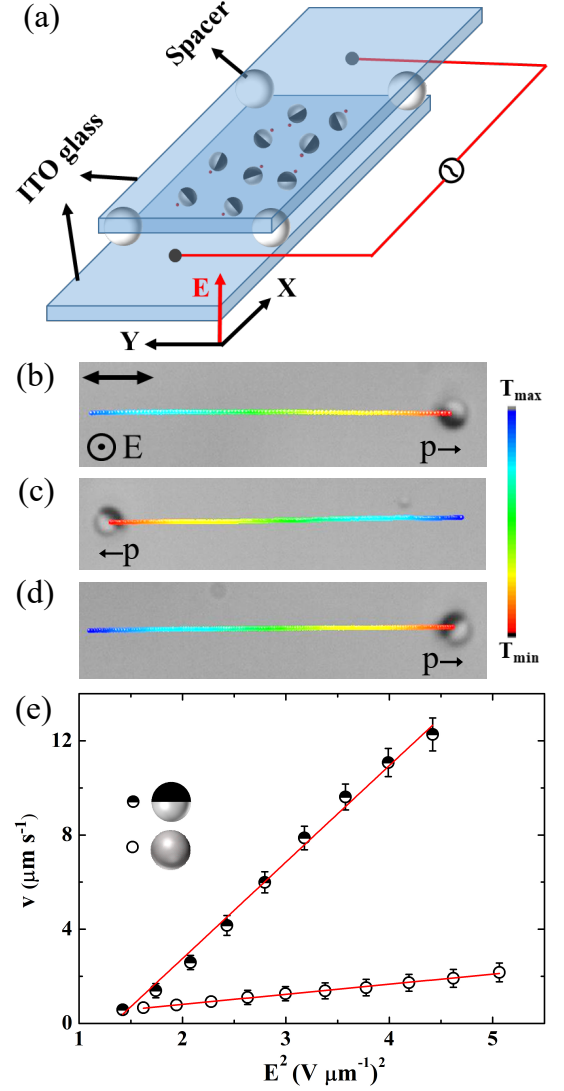


FIG. 4. (a) Diagram of a cell for applying electric field orthogonal to the director  $\hat{n}$ .  $\mathbf{E}$  is along the  $z$ -axis and the director is along the  $x$ -axis. (b-d) Time coded trajectories of a few Janus dipolar particles in MLC-6608 liquid crystal with different orientations of the metal hemisphere under the field amplitude of  $2.0 \text{ V}/\mu\text{m}$  at  $30 \text{ Hz}$  (see Movie S2).  $T_{\text{max}} = 5 \text{ s}$ ,  $T_{\text{min}} = 0 \text{ s}$ . Note that the direction of motion is antiparallel to elastic dipole  $\vec{p}$ . (d) Electric field dependent velocity ( $v$ ) of a Janus and non-Janus dipolar particle. Red lines represent linear fits to  $v \propto E^2$  with slopes  $4.1$  and  $0.4 \mu\text{m}^3 \text{s}^{-1} \text{V}^{-2}$  for the Janus and the non-Janus particles, respectively.



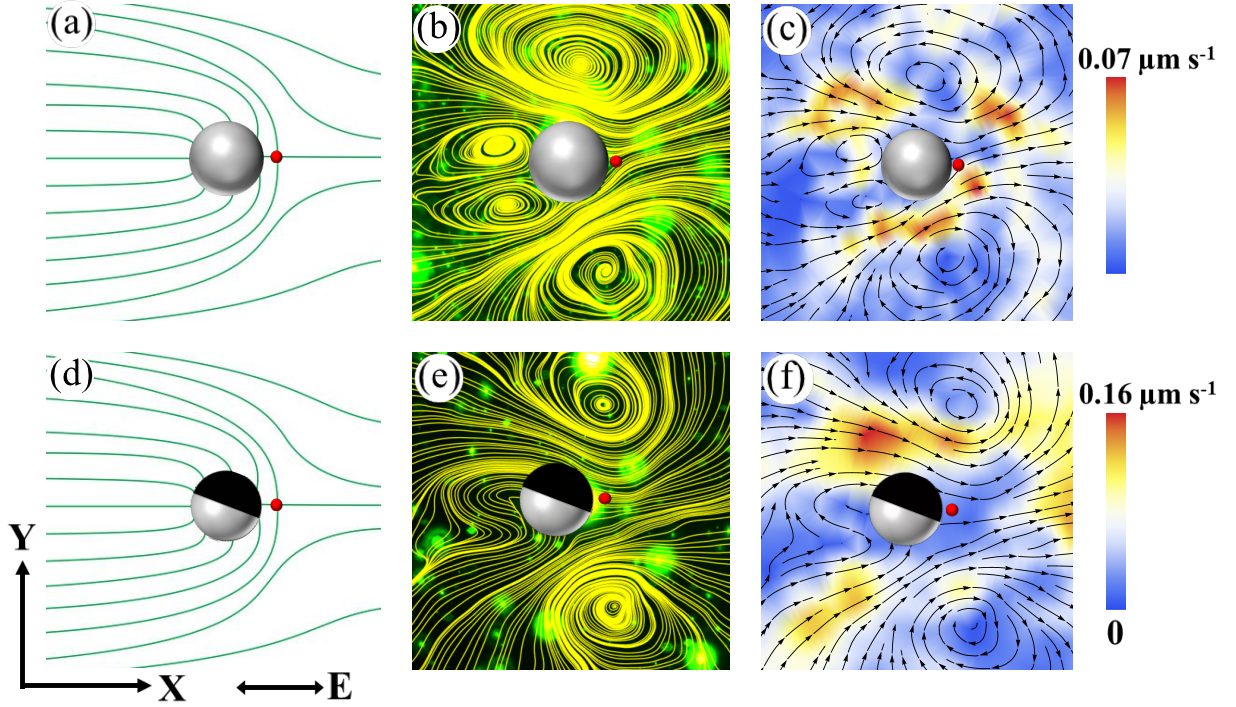


FIG. 5. (a,d) Director profile around a Janus and non-Janus particles. The applied electric field is parallel to the director i.e., along the  $x$ -axis. (b) Streamlines of LC flow around a dipolar non-Janus particle. (c) Directional streamlines i.e., the velocity map of the LCEO flows around the non-Janus dipolar particle. (e) Streamlines of LC flow around a dipolar Janus particle. (f) The velocity map of the LCEO flow around the Janus dipolar particle. Field amplitude:  $9.0 \text{ mV}\mu\text{m}^{-1}$ , frequency: 30 Hz.

In what follows we studied the mobility of the Janus dipolar particles in a nematic mixture (MLC-6608) which has a negative dielectric anisotropy. In this sample, the electric field is applied perpendicular to the director  $\hat{n}$  as shown in Fig. 4(a). Figures 4(b-d) show time coded trajectories (representative) of three Janus dipolar particles with different orientations under the action of an ac electric field (see Movies S2) [40]. In this cell, the particles move along the director, similar to the previous cell (see Figs.3(a-d)) but they move leading the point defect i.e. the direction of motion is antiparallel to the elastic dipole  $\vec{p}$ . This is expected as the quantity in the parenthesis of equation (2) i.e.,  $(\Delta\epsilon/\bar{\epsilon} - \Delta\sigma/\bar{\sigma} = -1.54)$  is negative [40]. Figure 4(e) shows the field dependent velocity of a Janus and non-Janus particle. We notice that the Janus particles move faster as compared to the non-Janus particles. For example, at  $E^2 = 4.0 \text{ (V}/\mu\text{m})^2$ , the velocity of the Janus particle is  $v_J = 11 \mu\text{m/s}$  and the velocity of the non-Janus particle is  $v = 1.6 \mu\text{m/s}$ .

In both the samples the velocity of the Janus dipolar particles is much higher than that of the non-Janus particles and this can be quantitatively understood based on the electroosmotic flows surrounding the particles. We have used the  $\mu$ -PIV technique to observe the electroosmotic flows in 5CB LC [42]. For this purpose, we have chosen a bigger particle of diameter  $50 \pm 4 \mu\text{m}$  and fixed it with a glue in the middle of the cell. The gap between

the two in-plane electrodes is 4 mm. A small quantity (0.01wt%) of CdSe/Zn fluorescent quantum dots (QDs) of size 1-2 nm are dispersed in the LC and used as tracer particles. The absorption maximum of the QDs is 512 nm and the emission wavelength is in the range of 530-550 nm. In the presence of the ac field the QDs follow the electro-osmotic flows. The movie of the flows is recorded using a Ni-S2 (Nikon) colour camera exposed at 300 ms with a rate of one frame per second. The recorded file is saved as an array of images and analysed using  $\mu$ -PIV software [42]. The final flow pattern is obtained after averaging over nearly 100 images.

Figures 5 (b) and (e) show the flow map around a non-Janus and a Janus dipolar particle. The non-Janus particle exhibits asymmetric quadrupolar flows as expected. Two bigger vortices are formed adjacent to the point defect and the smaller vortices are formed on the opposite side and the fore-aft symmetry of the electroosmotic flow is broken due to the point defect. Corresponding directional flow (Fig.5(c)) suggests that the flow is outward along the director, similar to that of “Pusher” type micro-swimmers. However, the flow field of the Janus particle is somewhat different. In particular, two small vortices on the left side of the microsphere are incomplete and it looks more like a dipolar type flow. More importantly the velocity of the fluid near the metal hemisphere is much higher than that of the silica hemisphere



(see colour coded bar). For example, the maximum electroosmotic velocity for the non-Janus particle is  $0.07 \mu\text{m/s}$  whereas the maximum velocity for the Janus particle is  $0.16 \mu\text{m/s}$ , i.e., nearly double (Fig.5(f)). This is expected as the polarisability of the metal hemisphere is much larger than that of the dielectric and the induced charge density for the Janus particle is larger. Using Eq.(2) and considering  $\bar{\eta}_{LC} \approx 90 \text{ mPas}$ ,  $E = 9 \text{ mV}/\mu\text{m}$ ,  $R=25 \mu\text{m}$  and the calculated dielectric and conductivity anisotropies [40], we estimate the electroosmotic flow velocity for the non-Janus particle in 5CB LC is  $u_{max} \approx 0.05 \mu\text{m/s}$ . This is very close to the value measured in the experiments (Fig.5(c)).

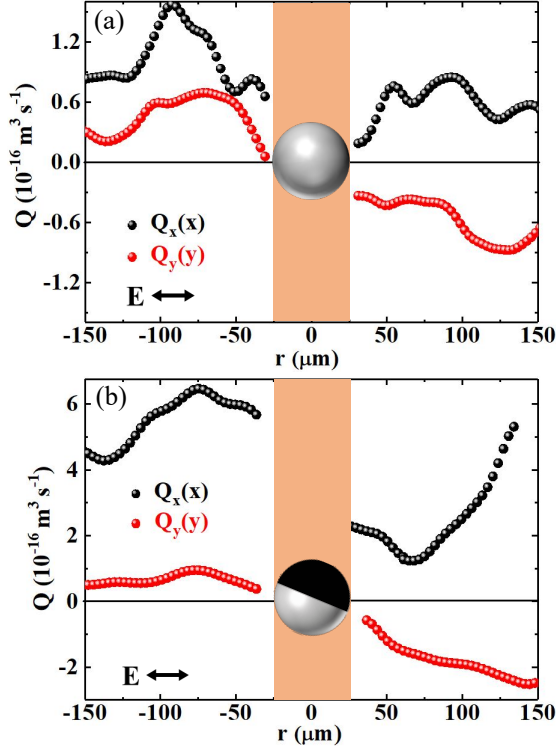


FIG. 6. Volumetric flow functions  $Q_x(x)$  and  $Q_y(y)$  for the (a) non-Janus and (b) Janus particles. Pumping of LC is from the left to the right direction.

We have also calculated the volumetric flows  $Q_x(x)$  and  $Q_y(y)$ , that estimates the pumping of fluid around the sphere passing through the  $yz$  cross-section of the cell which can be written as [34]:

$$Q_x(x) = \frac{2}{3}h \int_{-y_0}^{y_0} u_x(x,y)dy \quad (3)$$

$$Q_y(y) = \frac{2}{3}h \int_{-x_0}^{x_0} u_y(x,y)dx \quad (4)$$

where  $u_x(x,y)$  and  $u_y(x,y)$  are velocity components

known from the experiments,  $h$  is thickness of the cell and  $x_0 = y_0 = 150 \mu\text{m}$ .  $Q_x(x)$  and  $Q_y(y)$  for both the non-Janus and Janus particles are shown in Fig.6(a) and (b), respectively. For the non-Janus particle,  $Q_x$  is positive on both sides of the particle that means the LC is pumped from left to right whereas,  $Q_y$  is positive and negative across the particle which means fixing of flows with no net pumping of fluid along the  $y$ -direction. For the Janus particle, the response is similar but the maximum  $Q_x$  value is much larger than that of the non-Janus particle. It means that, comparatively the pumping of fluid from the left to the right is more for the Janus particle and the stronger pumping is responsible for higher velocity.

It may be mentioned that for the Janus quadrupolar particles, the outside medium is symmetric (director profile) and the asymmetry of the particle breaks the fore-aft symmetry of electroosmotic flows [35, 36]. In case of Janus dipolar particles, the medium is asymmetric and the fore-aft symmetry of the flows is broken due to the medium as well the particle. Since the motion of the Janus dipolar particles is restricted along the director, the electroosmosis due to the asymmetric medium is dominant.

#### IV. CONCLUSION

We have shown that the direction of motion of Janus dipolar particles is parallel to the direction of the elastic dipoles in 5CB and antiparallel in MCL-6608. The velocity of the Janus particles is much higher than that of the non-Janus particles in both 5CB and MLC-6608. We have mapped the flow fields in 5CB using  $\mu$ -PIV and observed quadrupolar flows around the non-Janus particle, whereas the small vortices are obscured and nearly a dipolar type flows are observed in case of the Janus particles. The electroosmotic flows on the metal hemisphere is almost two times higher compared to the dielectric hemisphere. Stronger flows on metal hemisphere could be responsible for obscuring the small vortices and showing dipolar like flows. The volumetric flow of fluid along the direction of motion for the Janus particle is stronger than that of the non-Janus particles. Our study shows that for a given liquid crystal the motility of the particles can be enhanced by making the surface asymmetric without adjusting the dielectric and conductivity anisotropies. Janus particles with asymmetric shape, higher order elastic moment and genus could offer unusual motility and dynamics in liquid crystals.

**Acknowledgments:** SD acknowledges the support from the Department of Science and Technology, Govt. of India (DST/SJF/PSA-02/2014-2015), DST-PURSE-II and UoH (UoH/IoE/RC1-20-010). DKS acknowledges DST INSPIRE fellowship.

- 
- [1] C. Bechinger, R. D. Leonardo, H. Löwen, C. Reichhardt, G. Volpe, and G. Volpe, *Rev. Mod. Phys.* **88**, 045006 (2016).
- [2] J. Wang, and W. Gao, *ACS Nano* **6**, 5745 (2012).
- [3] H. R. Jiang, H. Wada, N. Yoshinaga, and M. Sano, *Phys. Rev. Lett.* **102**, 208301 (2009).
- [4] H. R. Jiang, N. Yoshinaga, and M. Sano, *Phys. Rev. Lett.* **105**, 268302 (2010).
- [5] G. Li and J. X. Tang, *Phys. Rev. Lett.* **103**, 078101 (2009).
- [6] D. Nishiguchi, and M. Sano, *Phys. Rev. E* **92**, 052309 (2015).
- [7] H. R. Vutukuri, M. Lisicki, E. Lauga and J. Vermant, *Nat. Commun.* **11**, 2628 (2020).
- [8] S. Thutupalli, R. Seemann, and S. Herminghaus, *New J. Phys.* **13**, 073021 (2011).
- [9] P. Tierno, R. Golestanian, I. Pagonabarraga, and F. Sagués, *Phys. Rev. Lett.* **101**, 218304 (2008).
- [10] S. Ramaswamy, *Annu. Rev. Condens. Matter Phys.* **1**, 323 (2010).
- [11] M. C. Marchetti, J. F. Joanny, S. Ramaswamy, T. B. Liverpool, J. Prost, M. Rao, and R. A. Simha, *Rev. Mod. Phys.* **85**, 1143 (2013).
- [12] I. S. Aranson, *Phys. Usp.* **56**, 79 (2013).
- [13] E. Lauga and T. R. Powers, *Rep. Prog. Phys.* **72**, 096601 (2009).
- [14] A. Ramos, *Electrokinetics and Electrohydrodynamics in Microsystems* (Springer, 2011).
- [15] H. Morgan and N. G. Green, *AC Electrokinetics: Colloids and nanoparticles* (Research Studies Press Ltd, 2003).
- [16] J. Yan, M. Han, J. Zhang, C. Xu, E. Luijten, and S. Granick, *Nat. Mater.* **15**, 1095 (2016).
- [17] B. Comiskey, J.D. Albert, H. Yoshizawa, and J. Jacobson, *Nature* **394**, 253 (1998).
- [18] R. C. Hayward, D. A. Saville, and I. A. Aksay, *Nature* **404**, 56 (2000).
- [19] S. Gangwal, O. J. Cayre, M. Z. Bazant, and O. D. Velev, *Phys. Rev. Lett.* **100**, 058302 (2008).
- [20] M. Fuduo, Y. Xingfu, Z. Hui, and N. Wu, *Phys. Rev. Lett.* **115**, 208302 (2015).
- [21] V.A. Murtsovkin, *Colloid Jour.* **58**, 341 (1996).
- [22] T. M. Squires and S. R. Quake, *Rev. Mod. Phys.* **77**, 977 (2005).
- [23] M. Z. Bazant, M.S. Kilic, B.D. Storey, and A. Ajdari, *Adv. Colloid Interface Sci.* **152**, 48 (2009).
- [24] T. M. Squires and M. Z. Bazant, *J. Fluid Mech.* **509**, 217 (2004).
- [25] M.Z. Bazant and T. M. Squires, *Phys. Rev. Lett.* **92**, 066101 (2004).
- [26] T.M. Squires and M. Bazant, *J. Fluid Mech.* **560**, 65 (2006).
- [27] O. D. Lavrentovich, I. Lazo, and O. P. Pishnyak, *Nature* **467**, 947 (2010).
- [28] I. Lazo and O. D. Lavrentovich, *Phil. Trans. Soc. A* **371**, 2012255 (2013).
- [29] O. D. Lavrentovich, *Curr. Opin. Colloid Interface Sci.* **21**, 97 (2016).
- [30] O. D. Lavrentovich, *Soft Matter* **10**, 1264 (2014).
- [31] O.P. Pishnyak, S. Tang, J. R. Kelly, S.V. Shiyankovskii, and O.D. Lavrentovich, *Phys. Rev. Lett.* **99**, 127802 (2007).
- [32] S. Hernández-Navarro, P. Tierno, J. A. Farrera, J. Ignés-Mullol, and F. Sagués, *Angew. Chem. Int. Ed.* **53**, 10696 (2014).
- [33] A. V. Straube, J. M. Pagés, P. Tierno, J. Ignés-Mullol, and F. Sagués, *Phys. Rev. Res.* **1**, 022008(R) (2019).
- [34] I. Lazo, C. Peng, J. Xiang, S. V. Shiyankovskii, and O. D. Lavrentovich, *Nat. Commun.* **5**, 5033 (2014).
- [35] D. K. Sahu, S. Kole, S. Ramaswamy and S. Dhara, *Phys. Rev. Res.* **2**, 032009(R) (2020).
- [36] D. K. Sahu, and S. Dhara, *Phys. Rev. Applied.*, **14**, 034004 (2020).
- [37] D. K. Sahu, and S. Dhara, *Phys. Fluids* **33**, 0187106 (2021).
- [38] I. Mušević, *Liquid crystal colloids*. 2017. (Springer International Publishing AG).
- [39] I. I. Smalyukh, *Annu. Rev. Condens. Matter Phys.* **9**, 207 (2018).
- [40] Supplemental Information for materials data and description of movies.
- [41] S. Paladugu, C. Conklin, J. Viñals, and O. D. Lavrentovich, *Phys. Rev. Appl.* **7**, 034033 (2017).
- [42] W. Thielicke and E. J. Stamhuis, *Time Resolved Digital Particle Image Velocimetry Tool for MATLAB*. <http://pivlab.blogspot.com/p/pivlabdocumentation.html> (2010).

**ACKNOWLEDGEMENTS:** This work is supported by the DST, Govt. of India (DST/SJF/PSA-02/2014-2015) and University of Hyderabad (UoH/IoE/RC1- 20-010). DKS acknowledges INSPIRE Fellowship from the DST. We also thank K.V. Raman for help in preparing Janus particles.